First-principles study of adsorption, diffusion, and charge stability of metal adatoms on alkali halide surfaces

M. H. Hakala, O. H. Pakarinen, and A. S. Foster
Laboratory of Physics, Helsinki University of Technology, P.O. Box 1100, FIN-02150 HUT, Finland
(Received 6 May 2008; published 16 July 2008)

In this work we have performed first-principles calculations based on the spin-polarized density-functional theory for the adsorption and diffusion of Au, Ag, and Pb atoms on NaCl(001), KCl(001), and KBr(001) surfaces. We consider also the influence of adatom charge on the adsorption and diffusion. In order to characterize the different systems we explicitly calculate charge transfer between surface and adatom and consider the relative stability of the various charge states. Our results show that in general, apart from positively charged systems, the adatoms are weakly bound to the surface via orbital polarization and ionic interactions, and relatively little charge transfer occurs. Au and Ag adatoms are highly mobile on all surfaces, although they can be pinned by removal of an electron. In contrast, Pb adatoms are fairly immobile, and their mobility increases upon charging. Analysis of the charge stability suggests that Ag offers the potential of charge controlled mobility on insulators.

DOI: 10.1103/PhysRevB.78.045418 PACS number(s): 68.43.Jk, 63.20.dk, 68.35.Fx

I. INTRODUCTION

The study of adatom adsorption and diffusion on crystal surfaces remains an important step in predicting the growth properties of deposited material, particularly for understanding the kinetic processes that dominate growth away from equilibrium.[1] The adsorption of metal adatoms onto insulating surfaces and thin films has become a key focus in this area due to the importance of understanding the catalytic properties of metallic nanoclusters adsorbed on insulating surfaces.[2–4] Alongside understanding the growth and formation of these nanoclusters, an important avenue of research is the study of how charge transfer between the surface and adsorbed atoms influences the nanocluster's reactivity. Recent studies have characterized the bonding and charge transfer of Au atoms on MgO (001) thin films[5–7] and shown how these can be controlled by changing the thickness of the film.[8,9]

Experimental characterization of these systems is often performed via scanning probe microscopy (SPM) and scanning tunneling microscopy (STM) (Ref. 10) experiments have been able to identify[8] and even manipulate[11,12] the charge state of adsorbed Au and Ag adatoms on MgO and NaCl (001) thin films. As well as providing insight into the unexpected reactivity of these systems, the capability of charge measurement and control is a key to the development of practical molecular scale electronics.[13] Although thin-film systems are important in themselves, it is well known that their properties can differ significantly from bulk insulators,[9] and characterization on bulk insulating surfaces is equally important. For these fully insulating systems tunneling measurements are not possible and STM cannot be used, hence high-resolution SPM studies require noncontact atomic force microscopy (NC-AFM).[14–17] NC-AFM is only recently being applied to the study of metal/insulator systems, and high-resolution studies have been published only for Au on RbI (001) and KBr (001) surfaces,[18–20] and Pd on the MgO (001) surface.[21]

The kinetic properties of adsorbed adatoms and molecules can also be probed via SPM mechanical manipulation, providing a direct link to the diffusion barriers of adsorbed species. This approach has a long history in STM on conducting surfaces[22] but is relatively new for AFM on insulators. Very recently NC-AFM has been used to manipulate individual adatoms on several semiconducting surfaces,[23–25] and for defects on KCl (001) surfaces[26] and adsorbed molecules on CaF_2 (111) surfaces.[27] An extension to the study of the manipulation of metal adatoms and nanoclusters on insulators is an obvious next step, but as yet experiments have not been successful. In this work, we use first-principles simulations to study the interaction of metal adatoms with different alkali halide surfaces and provide predictions for adsorption strength, spin, charge stability, and diffusion that are crucial in understanding and designing experiments on these benchmark systems. Earlier attempts to theoretically characterize metal adsorption on alkali halides demonstrated the ability of calculations to help in explaining experiments[28,29] but focused on a smaller set of systems and properties and also showed that the simpler theoretical models used cannot capture the full interaction between all adatoms and surfaces.

II. METHODS

The calculations were performed using the linear combination of atomic orbitals basis SIESTA code,[30,31] implementing the spin-polarized density-functional theory (DFT) within the generalized gradient approximation. We use the functional of Perdew, Burke, and Ernzerhof.[32] Core electrons are represented by norm-conserving pseudopotentials using standard Troullier-Martins parametrization, including partial core and scalar relativistic corrections. The pseudopotential for Cl was generated in the electron configuration $[Ne]3s^2 3p^5$, Br in $[Ar\ 3d^{10}]4s^2 4p^5$, Na in $[Ne]3s^1$, K in $[Ar]4s^1$, Ag in $[Kr]5s^1 4d^{10}$, Au in $[Xe\ 4f^{14}]6s^1 5d^{10}$, and Pb in $[Xe\ 4f^{14} 5d^{10}]6s^2 6p^2$ with the core electrons given in square brackets. The basis set for each system was optimized to provide high accuracy and flexibility: double ζ with polarization for $Na(3s^1)$, $Cl(3p^5)$, $K(4s^1)$, $Br(4p^5)$, $Ag(4d^{10})$, $Au(5d^{10})$, $Pb(6s^2)$, double ζ for $Cl(3s^2)$, $Br(4s^2)$, and triple ζ

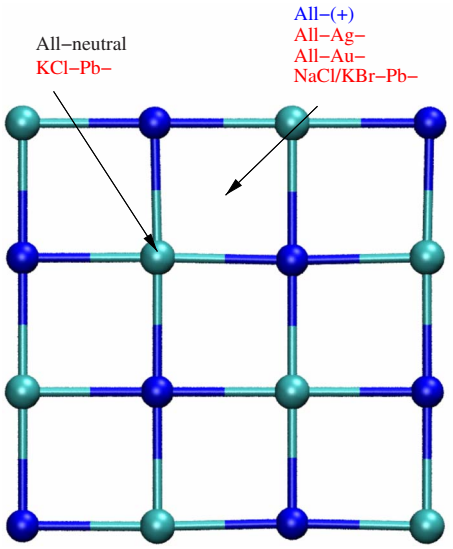

FIG. 1. (Color online) Minimum energy sites for adatoms over the substrates. Anions (Cl, Br) are colored light blue (light gray) and cations (Na, K) are dark blue (dark gray).

with double polarization for Ag($5s^1$), Au($6s^1$), and Pb($6p^2$). The system's properties were converged with respect to k points ($1\times2\times2$ grid[33]) and mesh (corresponding to an energy cutoff of 175 Ry.). The chosen energy shifts corresponded to maximum cutoffs of $9.02a_0$ for Ag, $8.21a_0$ for Au, $9.42a_0$ for Pb, $12.56a_0$ for K, $6.65a_0$ for Br, $6.15a_0$ for Cl, and $11.05a_0$ for Na. This setup resulted in bulk lattice constants of the materials within a few percent of experiment.[34] Calculated atomic electron affinities (AEs) and ionization potentials (IPs) for Au, Ag, and Pb provide an accuracy comparable to previous DFT studies.[35,36] The AE and IP values for Au and Ag, and the IP for Pb are also in good agreement with experiment.[34] The electron affinity for Pb differs significantly from the published experimental value [0.35 eV (Ref. 37)], but calculations at the MP2 (1.40 eV) and CCSD (1.07 eV) level[38] give similar values to our SIESTA calculations and suggest that the experimental number is for a different transition.

Our surfaces were represented by a 2×2 conventional unit-cell slab model (see Fig. 1) with a large enough vacuum in the (100) direction to remove any interaction between periodic images. We found that depth of three atomic layers of NaCl, KCl, and KBr was enough to converge the surface relaxations. The bottom layer of substrate was fixed during all the molecular relaxation calculations to represent the bulk, while all other atoms were allowed to relax. All the structural relaxations were performed using conjugate gradient method and unconstrained forces were relaxed below 0.02 eV/Å. For the diffusion barrier, metal atoms were dragged a small step in the selected direction (100/110). For each step the substrate was fully relaxed and metal atom was relaxed in the plane perpendicular to the selected direction. Charged systems were calculated by adding/removing an electron and applying a compensating background charge density. Adsorption energies were calculated with respect to the isolated surface and atom [the ground state of all atoms was spin-polarized: Au, Ag($s=\frac{1}{2}$), and Pb($s=1$)] and include counterpoise corrections[39] for basis-set superposition errors. Total energies for charged species have been corrected to first order with respect to the artificial electrostatic interaction between periodic cells.[40,41]

III. RESULTS

A. Absorption

The calculated adsorption sites are shown in Fig. 1 and values for absorption energies are shown in Table I. In order to investigate the charge transfer between adsorbing atoms and the substrate, we also used Mulliken population analysis[42] and calculated the induced charge density.[43] The latter is defined as the difference between the complete adsorbate+surface system and the neutral systems of atom and substrate,

$$\rho_{\mathrm{ind}} = \rho(\mathrm{atom/ion} + \mathrm{substrate}) - \rho(\mathrm{substrate}) - \rho(\mathrm{atom/ion}). \tag{1}$$

As discussed previously, charge transfer is a key characteristic in understanding the structure and reactivity of metallic adsorbates and is a useful method for characterizing the binding mechanism. The ionic charges given by Mulliken analysis are shown in Table II and the induced charge transfer is shown in detail for key systems in Figs. 2–4. Note that both these approaches for analysis of the charge transfer are qualitative and useful for comparing between systems but cannot be used to calculate the absolute values of charge transfer.

The absorption site for Au was found to be on top of the anion site for all the substrates. The Au-anion distance was around 2.65 Å in all cases and no significant relaxation of substrate atoms was observed [see Fig. 2(a)]. Table II shows that there is some charge transfer to the Au adatom on all substrates, although it is quite small. For charged systems the minimum-energy sites for Au^- and Au^+ systems were found to lie in the hollow site on the surface. As for the neutral case, Au^- leaves the surface rather unperturbed—Au^- is also almost fully saturated by the additional electron, and we observed a significant reduction in induced charge density [see

TABLE I. Absorption energies in eV.

	Ag	Au	Pb	Ag^-	Au^-	Pb^-	Ag^+	Au^+	Pb^+
NaCl	−0.23	−0.45	−0.59	−1.64	−1.97	−1.47	−1.81	−3.77	−2.11
KCl	−0.34	−0.65	−0.83	−2.44	−2.61	−1.66	−3.17	−5.10	−2.69
KBr	−0.34	−0.70	−0.80	−2.31	−2.48	−1.60	−3.46	−5.46	−2.85

TABLE II. Ionic charge with respect to the neutral atom at equilibrium position (e). During the diffusion these values remain almost constant.

	Ag	Au	Pb	Ag^-	Au^-	Pb^-	Ag^+	Au^+	Pb^+
NaCl	−0.003	0.075	0.011	0.486	0.388	0.577	−0.554	−0.260	−0.599
KCl	0.041	0.138	0.093	0.600	0.590	0.639	−0.402	−0.108	−0.442
KBr	0.033	0.172	0.126	0.436	0.580	0.594	−0.290	+0.002	−0.357

Fig. 3(a), and note the reduced scale]. For Au^+ there was a large relaxation at the surface with the adatom bonding closer to the surface and clear upward displacement of neighboring Cl/Br atoms [see Fig. 4(a)]. The induced charge-density plots for Au^+ systems shows a large depletion of neighboring anions and accumulation at the adsorption site. This is also reflected in the small difference in ionic charge from the neutral atom seen for Au^+ (see Table II). The resultant distance between Au^+ and the surface is about 1.5, 1.4, and 1.2 Å for NaCl, KCl, and KBr, respectively (see Fig. 4).

Our calculated adsorption energy of 0.45 eV for the neutral adatom is in good agreement with experimental estimates of 0.49 eV (Refs. 1, 44, and 45)—this agreement

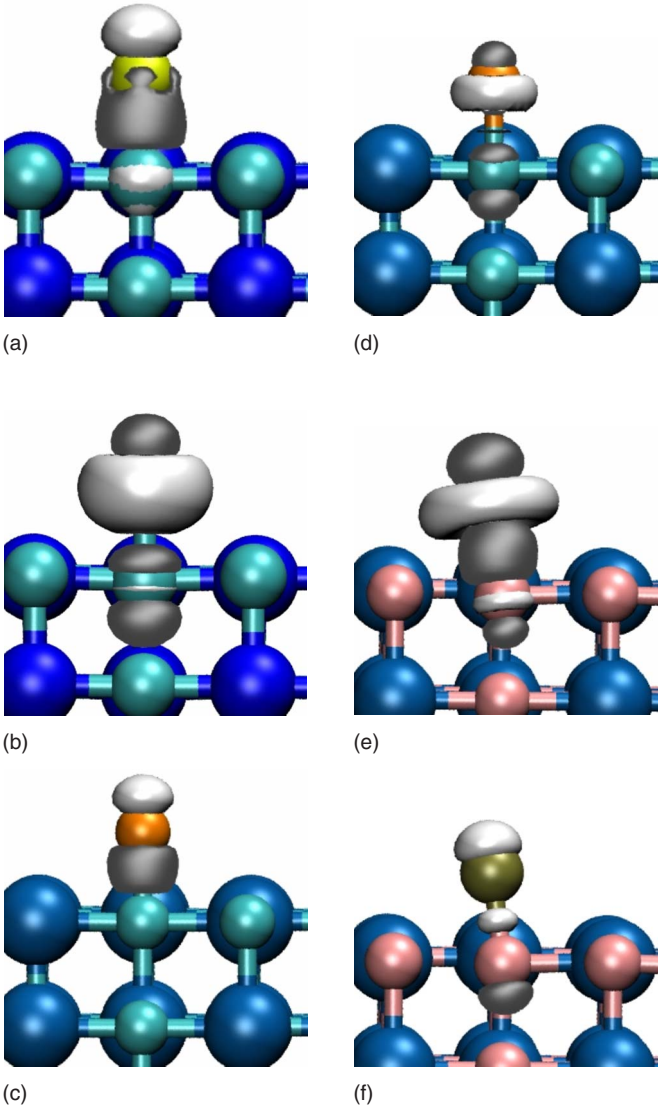

FIG. 2. (Color online) Spin-up (a, c, e) and spin-down (b, d, f) induced charge-density isosurfaces for (a, b) Au^0 on NaCl, (c, d) Ag^0 on KCl and (e, f) Pb^0 on KBr. In the atomic structures, Na is blue, K is blue/gray, Cl is cyan, Br is pink, Au is yellow, Ag is orange and Pb is brass. Accumulated charge is plotted as a light gray isosurface (+0.001 Hartree/Bohr) and depleted charge is dark gray (−0.001 Hartree/Bohr).

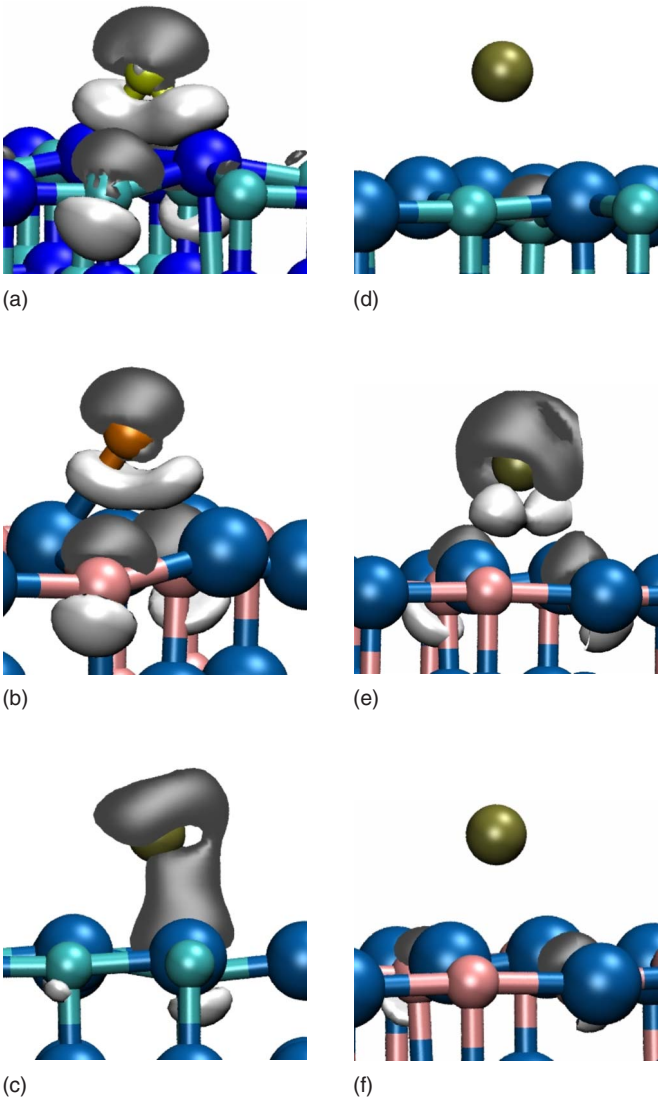

FIG. 3. (Color online) Spin-up (a, b, c, e) and spin-down (d, f) induced charge-density isosurfaces for (a) Au^- on KBr, (b) Ag^- on KBr and (c, d) Pb^- on KCl and (e, f) Pb^- on KBr. Charge density isosurfaces are plotted at ±0.0004 Hartree/Bohr.

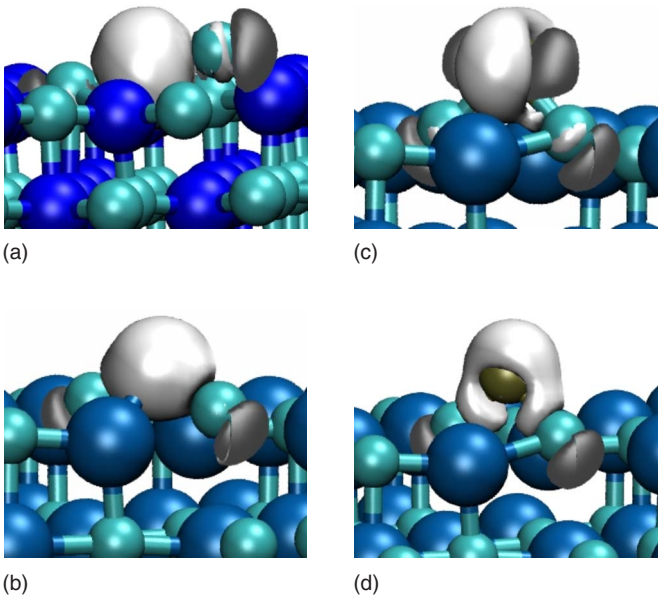

FIG. 4. (Color online) Induced charge-density isosurfaces for (a) Au^+ on NaCl and (b) Ag^+ on KCl, (c) spin-up and (d) spin-down Pb^+ on KCl. Charge density isosurfaces are plotted at ± 0.001 Hartree/Bohr.

should not be treated too seriously since it is difficult to isolate the contribution of the surface terraces in experiments. We can also compare to recent results for NaCl thin films on Cu,[11] where Au was found to adsorb on top of Cl at a distance of 3.2 Å with a bonding energy of 0.4 eV. However, they found a similar adsorption site for Au^- in contrast to our results, reflecting the role of the metal substrate in stabilizing the charged state.

The absorption site for neutral Ag was on top of the anion site with Ag-anion distances of 2.84, 2.81, and 2.86 Å for NaCl, KCl, and KBr, respectively. No significant relaxation of the substrate is observed, and the resultant charge transfer from the surface is significantly less than for Au and practically zero. For charged systems we find that the minimum-energy sites are in hollow sites, as for Au, and a small perturbation in the substrate is observed only for Ag^+ systems on KCl and KBr. Accumulation on Ag^+ is also smaller than for Au^+, particularly on NaCl (compare NaCl-Ag^+ and KCl-Au^+ in Fig. 4). This is also reflected in the distance between Ag^+ and the surface, which changes little from the neutral case for NaCl but reduces to 1.98 and 1.81 Å for KCl and KBr, respectively.

We reproduce the reduction in adsorption energy for Ag in comparison to Au, but the experimental estimate of 0.41 eV (Refs 1, 44, and 45) is a little larger than our calculated value of 0.23 eV. Again, we can also compare our results to an experimental and computational study on NaCl thin films.[12] In reasonable agreement with our calculations, they found that neutral Ag adsorbs on top of the Cl^- anion with an adsorption energy of 0.11 eV at a distance of 3.0 Å, while Ag^+ is found in the hollow site. However, as for Au^-,[11] Ag^- remained at the anion site for the thin-film system, while we predict that both charged states prefer the hollow site. This is likely caused by interaction with the metal substrate, but the use of LDA+U to force the localization of the added electron onto the metal atom is also a significant deviation from our approach.

As for Au and Ag, neutral Pb adsorbed at the anion site for all substrates with an anion-Pb distance of 2.87, 2.78, and 2.90 Å for NaCl, KCl, and KBr, respectively. No significant relaxation of the substrate is observed, and the resultant charge transfer from the surface lies roughly in between the transfer Au and Ag. All charged adatoms adsorbed at the hollow site, except for Pb^- on KCl, where the lowest energy site is over an anion—here we see only depletion at the adatom [see Fig. 3(b)] and the bond length increases to 3.24 Å.

1. Charge transfer and bonding character

In general, for all neutral systems the charge transfer from the surface to the metal atom is very small and is effectively zero for Ag and all adatoms on NaCl (see Table II). The magnitude of this charge transfer correlates exactly with the electronegativity of the constituent elements. Among the metals Au is the most electronegative (2.54 on the Pauling scale[46]), followed by Pb (2.33), Ag (1.93), and then much lower values for Na (0.93), and then K (0.82). The halides are among the most electronegative elements, and both Cl (3.16) and Br (2.96) have high values. The largest charge transfer should be seen for the most electronegative metal adatom on the least ionic surface, i.e., Au on KBr, and the smallest for the least electronegative metal adatom on the most ionic surface i.e., Ag on NaCl—this is exactly what is shown in Table II.

Although the charge transfer can be understood quite simply, the actual strength of bonding between adatom and the surface is a more complex interplay of polarization, and ionic and covalent interactions. If we compare the NaCl-Pb, NaCl-Ag, and KCl-Au systems in Fig. 2, we immediately see that Au and Ag show a similar accumulation/depletion pattern (with a larger magnitude seen for Au), as would be expected since they have similar valence orbital character. The patterns indicate a polarization of the metal atoms orbitals and a small accumulation on the *s* orbital of the surface anion with a corresponding depletion of the density in the bond area—characteristic of the formation of an ionic bond. For Pb, the valence *p* orbital introduces a different pattern of polarization with accumulation also at the anion *p* orbital, but the interaction remains ionic. In contrast, positively charged metal adatoms desperately need an electron source, and in all cases they move very close to the surface and form covalent bonds. This can be clearly seen in the NaCl-Au^+ system in Fig. 4(a), where the adatom is in the same plane as surface Cl^- ions and we see strong accumulation at the adatom. As for the charge transfer, the strength on bonding is influenced by the electronegativity of the elements. For neutral atoms, Ag has lower adsorption energies than Au (see Table II) due to smaller charge transfer, but the accumulation at *p* orbitals in Pb provides the strongest ionic interaction. The differences in charge transfer across the surfaces means there is no direct correlation to surface ionicity for bonding of neutral species, although the adsorption energies are usually lower on NaCl. However, the role of the substrate can be clearly seen for the more covalent adsorption of positive

TABLE III. Energy constants for moving between charge states.

	Ag($q=-e$)	Ag($q=+e$)	Au($q=-e$)	Au($q=+e$)	Pb($q=-e$)	Pb($q=+e$)
NaCl $\Delta E(0\rightarrow q)$	0.96	8.72	−0.48	11.06	2.22	7.97
NaCl $\Delta E(q\rightarrow 0)$	0.21	−6.79	2.79	−7.49	−1.16	−5.63
KCl $\Delta E(0\rightarrow q)$	−0.32	8.65	−1.62	10.81	1.6	8.65
KBr $\Delta E(q\rightarrow 0)$	1.38	−6.01	3.61	−7.12	−0.79	−5.93
KBr $\Delta E(0\rightarrow q)$	−0.03	8.3	−1.31	10.43	1.4	8.29
KBr $\Delta E(q\rightarrow 0)$	0.99	−5.52	3.13	−6.68	−0.69	−5.66

metal adatoms, where the adsorption energies increase with decreasing surface ionicity.

2. Spin

Analysis of the spin of the various systems shows that it is independent of the substrate and is purely determined by metal species and charge state. Au and Ag have identical spin states, and their spin-dependent induced charge transfer is very similar. For Au^0 and Ag^0 $s=\frac{1}{2}$, and Figs. 2(a)–2(d) show that the spin density is dominated by accumulation in a polarized s orbital above the adatom. Similar behavior was seen in recent calculations of Au on MgO.[6] Effectively, the small charge transfer between surface and adatoms, and weak bonding leaves the adatoms in a similar spin-state to the isolated atoms. Addition or removal of an electron leaves only filled shells and $s=0$ for all charged states of Au and Ag (spin-up- and spin-down-induced charge densities are identical).

Neutral Pb adatoms adsorb with both valence p-electrons spin up and $s=1$, as for the isolated atom, and the form of this orbital can be clearly seen by the comparison of spin-up- and spin-down-induced charged density in Figs. 2(e) and 2(f). Addition or removal of an electron produces a corresponding change in the total spin $S=\frac{3}{2}$ for Pb^- and $s=\frac{1}{2}$ for Pb^+, correlated with the number of electrons in the $6p$ orbital.

3. Stability

In order to study the relative stability of the different adatom charge states on the surface we have calculated the energy costs of moving between charged and neutral atomic states.[12] Here the energy cost $\Delta E(0\rightarrow q)$ and $\Delta E(q\rightarrow 0)$ denote charging of adatom A^0 and neutralizing charged adatom A^q at fixed equilibrium ionic configurations, respectively. The energy cost is given by

$$\Delta E(0\rightarrow q)=\begin{cases}\Phi-A-\Delta E_{el} & \text{for } q=-1\\ I-\Phi-\Delta E_{el} & \text{for } q=+1,\end{cases} \tag{2}$$

$$\Delta E(q\rightarrow 0)=2\Delta E_{\text{ion}}-\Delta E(0\rightarrow q), \tag{3}$$

where A and I are the affinity and ionization energies of the free atom, respectively, ΔE_{el} and ΔE_{ion} are electron relaxation and ionic reorganization energies gained by charging the atom respectively, and Φ is the work function of the surfaces. The values of work function were obtained via calculating the averaged electrostatic potential in the vacuum.[47,48] The obtained values for work function were 4.98, 4.30, and 4.47 eV for NaCl, KCl, and KBr, respectively [experimental estimates give a value of 5.12 eV for NaCl (Ref. 49)]. Calculated values for charge transition barriers are shown in Table III.

For Ag on KCl and KBr the behavior is qualitatively the same with a significant barrier for neutralization of Ag^- and no barrier to negative charging. For Ag on NaCl there is a barrier between negatively charged and neutral Ag in both directions. On all substrates, positively charged Ag $\Delta E(q\rightarrow 0)$ is negative. These indicate that neutral Ag and Ag^- are stable on NaCl, Ag^- is stable on KCl/KBr, while Ag^+ will always relax to Ag^0 by acquiring an electron from the substrate. However, at room temperature the asymmetry of the barriers for negative charging/neutralizing on NaCl suggests that Ag^0 is the most probable state, in contrast to the other substrates. The electronegativity of Au means it prefers to be negatively charged on all surfaces, and it always gains energy when an electron is added. The behavior of Ag and Au with respect to charge stability is qualitatively similar to previous results for NaCl thin films, including the dependence on surface work function.[12] Pb adatoms are only stable in the neutral state with significant barriers to charging on all surfaces.

B. Diffusion

A summary of the lowest diffusion barriers for each metal-substrate system is given in Fig. 5. For neutral Au atoms, the diffusion is always in the 110 direction (path A in Fig. 6). The barrier on NaCl is almost zero, reflecting the weaker charge transfer and adsorption strength, but the barriers remain small, of the order of 0.1–0.2 eV, on the other substrates. Negatively charging Au has little effect on the size of the diffusion barriers, as they diffuse between hollow sites along the 100 direction (path C in Fig. 6) at a cost of less than 0.2 eV. In contrast, the increased charge accumulation and bonding of Au^+ to the substrates results in much larger diffusion barriers. This is particularly seen on NaCl, where the barrier increases to 0.8 eV, but barriers of 0.6 eV and 0.4 eV are seen for KCl and KBr, respectively.

The diffusion for neutral Ag on NaCl and KCl is along the 100 direction (path B in Fig. 6), while Ag diffuses via the 110 direction on KBr (path A in Fig. 6). The barriers are generally small with a maximum of just over 0.2 eV on KCl. Charging either positively or negatively has little significant

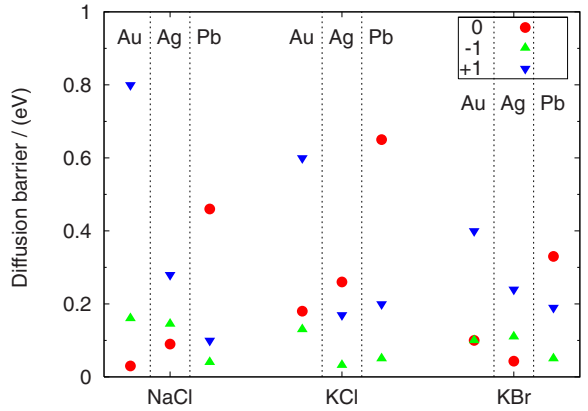

FIG. 5. (Color online) Diffusion barrier for Au, Ag and Pb adatoms on NaCl, KCl and KBr substrates. Three charged states ($\pm e$, neutral) are considered.

effect with all the barriers remaining near or below the value for neutral Ag on KCl. The reduced charge transfer and smaller size of the Ag adatom means that it can maintain equivalent bond strength during diffusion without strongly disrupting the surface.

Pb adatom diffusion is quite different to that of the other two metals and is the only case where significant diffusion barriers are found for the neutral case. On KCl and KBr, neutral Pb diffuses along the 110 direction (path A in Fig. 6), while on NaCl it diffuses along the 100 direction (path B in Fig. 6). The resultant barriers are about 0.5, 0.7, and 0.3 eV on NaCl, KCl, and KBr, respectively. Charging the Pb adatom reduces the barrier significantly on every surface. The behavior of Pb can be understood due to the specific bonding seen for the neutral atom with electron accumulation at parallel p orbitals in the adatom and anion, which is very site specific and cannot be reproduced during the diffusion. Charging of the Pb adatom also destroys this bond character (compare NaCl-Pb and KCl-Pb^- in Fig. 2), making it much easier for the adatom to diffuse. Across the substrates, the more localized charge density of NaCl generally results in higher barriers and the more covalent character of KBr reduces barriers, e.g., compare the barrier for Au^+ on each

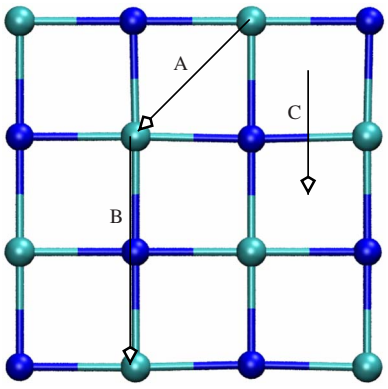

FIG. 6. (Color online) Schematic diagram of the diffusion paths. A is direct diffusion from a cation site to an other, B is in 100 direction over the anion site and C is the path over the bond from one bridging site to an other.

TABLE IV. Comparison of $E_a - E_d$ from different theoretical and experimental sources, where E_a is the absolute value of the adsorption energy and E_d is the diffusion barrier (eV).

	Ag	Au	Pb
NaCl	0.13,[a] 012,[b] 0.2[c]	0.42,[a] 0.08,[b] 0.4[c]	0.13[a]
KCl	0.09,[a] 0.2–0.3[c]	0.47,[a] 0.4[c]	0.18[a]
KBr	0.31,[a] 0.2–0.3[c]	0.60,[a] 0.2–0.4[c]	0.30[a]

[a]This work.
[b]Previous simulations (Ref. 29).
[c]Experiments (Ref. 45).

surface, but the correlations are not strong in every case.

A comparison of the combined data on adsorption and diffusion calculated in this work with previous simulations and experiments is shown in Table IV. The agreement shown is good for most systems, but we must be careful in comparing *ideal* theoretical results to experiments. Beyond the inherent errors of the calculation methodology, previous studies estimate that the error in comparing zero-temperature static internal energies in the calculations to finite temperature experimental enthalpies is about ± 0.1 eV.[50] Furthermore, experimental values may include contributions from nonterrace and defect sites, known to be preferential sites in cluster nucleation.[2]

IV. CONCLUSIONS

In summary, our calculations have demonstrated the limited role of charge transfer in the adsorption of metal adatoms on alkali halide surfaces and shown how the electronegativity of both adatoms and surface species dominates in the character and strength of the adatom-surface bond. For neutral and negatively charged atoms, the bonding is characterized by polarization of occupied orbitals and ionic interactions. The stronger adsorption of positively charged adatoms is seen in the significant displacement of surface ions and more covalent bonding character. We show that Au^- is the most stable state across all the surfaces considered, whereas Pb adatoms are unstable in either positive or negative charge states. Ag shows the weakest bonding but is more flexible in its charge state, demonstrating charge multistability on NaCl—although Ag^+ and all other positive metal adatoms are unstable. The generally weak interaction of Ag with all the surfaces means that it is highly mobile and this is fairly independent of its charge state. Au is also mobile in the neutral and negatively charged state but is more strongly pinned as Au^+. Pb adatoms show nearly opposite behavior, being immobile in neutral form, but highly mobile in either charged state.

If we consider SPM experiments, then at room temperature and depositing neutral atoms, only Pb atoms on NaCl and KCl are likely to remain on the terraces, and all other systems will see a rapid diffusion of atoms to more strongly bound sites. Hence, Pb is a viable candidate for exploring atomic manipulation on insulators at room temperature. At lower temperatures, studying the multiple charge states of Ag becomes possible, particularly on NaCl, but also on KBr.

However, the small differences in diffusion barriers between charge states on these substrates would make control extremely challenging and would likely require statistical evidence, rather than observation of single event. A more plausible approach might be to consider the role of low-coordinated and defect sites on the surface in the migration and charge stability of the adatoms and attempt to identify a promising candidate. Nevertheless, in general this kind experiment would parallel the study of charge state control already demonstrated on thin films[11,12] and open the door to the control of adatom mobility via charging. Direct injection of charge carriers into adatoms and molecules via the STM tip is a well-established technique, and the use of conducting tips would allow NC-AFM the same ability for studies on fully insulating samples.

ACKNOWLEDGMENTS

We acknowledge the generous computer resources from the Center for Scientific Computing, Espoo, Finland and as provided by the DEISA project. This research has been supported by the Academy of Finland through Project No. SA 211472. We wish to thank C. Barth and O. Custance for useful discussions. Induced charge-density plots were made using VMD.[51] We wish to thank Andris Gulans for useful discussions and benchmark calculations.

[1] J. A. Venables, G. D. T. Spiller, and M. Hanbücken, Rep. Prog. Phys. **47**, 399 (1984).
[2] C. R. Henry, Surf. Sci. Rep. **31**, 231 (1998).
[3] J. Libuda and H. J. Freund, Surf. Sci. Rep. **57**, 157 (2005).
[4] U. Heiz and U. Landman, *Nanocatalysis* (Springer-Verlag, Berlin, 2007).
[5] G. Pacchioni, L. Giordano, and M. Baistrocchi, Phys. Rev. Lett. **94**, 226104 (2005).
[6] M. Yulikov, M. Sterrer, M. Heyde, H.-P. Rust, T. Risse, H.-J. Freund, G. Pacchioni, and A. Scagnelli, Phys. Rev. Lett. **96**, 146804 (2006).
[7] L. Giordano and G. Pacchioni, Phys. Chem. Chem. Phys. **8**, 3335 (2006).
[8] M. Sterrer, T. Risse, U. M. Pozzoni, L. Giordano, M. Heyde, H.-P. Rust, G. Pacchioni, and H.-J. Freund, Phys. Rev. Lett. **98**, 096107 (2007).
[9] H.-J. Freund, Surf. Sci. **601**, 1438 (2007).
[10] G. Binnig and H. Rohrer, Helv. Phys. Acta **55**, 726 (1982).
[11] J. Repp, G. Meyer, F. E. Olsson, and M. Persson, Science **305**, 493 (2004).
[12] F. E. Olsson, S. Paavilainen, M. Persson, J. Repp, and G. Meyer, Phys. Rev. Lett. **98**, 176803 (2007).
[13] P. G. Piva, G. A. DiLabio, J. L. Pitters, J. Zikovsky, M. Rezeq, S. Dogel, W. A. Hofer, and R. A. Wolkow, Nature (London) **435**, 658 (2005).
[14] R. García and R. Pérez, Surf. Sci. Rep. **47**, 197 (2002).
[15] F. J. Giessibl, Rev. Mod. Phys. **75**, 949 (2003).
[16] W. Hofer, A. S. Foster, and A. L. Shluger, Rev. Mod. Phys. **75**, 1287 (2003).
[17] A. S. Foster and W. A. Hofer, *Scanning Probe Microscopes: Atomic Scale Engineering by Forces and Currents* (Springer, New York, 2006).
[18] O. H. Pakarinen, C. Barth, A. S. Foster, R. M. Nieminen, and C. R. Henry, Phys. Rev. B **73**, 235428 (2006).
[19] M. Goryl, F. Buatier de Mongeot, F. Krok, A. Vevecka-Priftaj, and M. Szymonski, Phys. Rev. B **76**, 075423 (2007).
[20] J. M. Mativetsky S. Fostner, P. G. Sarah, and A. Burke, Surf. Sci. **602**, L21 (2008).
[21] O. H. Pakarinen, C. Barth, A. S. Foster, and C. R. Henry, J. Appl. Phys. **103**, 054313 (2008).
[22] D. M. Eigler and E. K. Schweizer, Nature (London) **344**, 524 (1990).
[23] N. Oyabu, O. Custance, I. Yi, Y. Sugawara, and S. Morita, Phys. Rev. Lett. **90**, 176102 (2003).
[24] N. Oyabu, Y. Sugimoto, M. Abe, O. Custance, and S. Morita, Nanotechnology **16**, S112 (2005).
[25] Y. Sugimoto, M. Abe, S. Hirayama, N. Oyabu, O. Custance, and S. Morita, Nat. Mater. **4**, 156 (2005).
[26] R. Nishi, D. Miyagawa, Y. Seino, I. Yi, and S. Morita, Nanotechnology **17**, S142 (2006).
[27] S. Hirth, F. Ostendorf, and M. Reichling, Nanotechnology **17**, S148 (2006).
[28] J. A. Mejías, Phys. Rev. B **53**, 10281 (1996).
[29] J. H. Harding, A. M. Stoneham, and J. A. Venables, Phys. Rev. B **57**, 6715 (1998).
[30] J. Junquera, O. Paz, D. Sánchez-Portal, and E. Artacho, Phys. Rev. B **64**, 235111 (2001).
[31] J. M. Soler, E. Artacho, J. D. Gale, A. García, J. Junquera, P. Ordejón, and D. Sánchez-Portal, J. Phys.: Condens. Matter **14**, 2745 (2002).
[32] J. P. Perdew, K. Burke, and M. Ernzerhof, Phys. Rev. Lett. **77**, 3865 (1996).
[33] H. J. Monkhorst and J. D. Pack, Phys. Rev. B **13**, 5188 (1976).
[34] *Handbook of Chemistry and Physics*, 84th ed., edited by D. R. Lide (CRC, Boca Raton, 2003).
[35] L. Curtiss, P. Redfern, K. Raghavachari, and J. Pople, J. Chem. Phys. **109**, 42 (1998).
[36] Z. J. Wu and Y. Kawazoe, Chem. Phys. Lett. **423**, 81 (2006).
[37] C. S. Feigerle, R. R. Corderman, and W. C. Lineberger, J. Chem. Phys. **74**, 1513 (1981).
[38] R. A. Kendall, E. Apra, D. E. Bernholdt, E. J. Bylaska, M. Dupuis, G. I. Fann, R. J. Harrison, J. Ju, J. A. Nichols, J. Nieplocha, T. P. Straatsma, T. L. Windus, and A. T. Wong, Comput. Phys. Commun. **128**, 260 (2000).
[39] S. F. Boys and F. Bernadi, Mol. Phys. **19**, 553 (1970).
[40] G. Makov and M. C. Payne, Phys. Rev. B **51**, 4014 (1995).
[41] L. N. Kantorovich, Phys. Rev. B **60**, 15476 (1999).
[42] R. S. Mulliken, J. Chim. Phys. Phys.-Chim. Biol. **49**, 497 (1949).
[43] L. M. Molina and B. Hammer, Phys. Rev. B **69**, 155424 (2004).
[44] A. D. Gates and J. L. Robins, Appl. Surf. Sci. **48-49**, 154 (1991).
[45] J. A. Venables, Surf. Sci. **299-300**, 798 (1994).
[46] L. Pauling, *The Nature of the Chemical Bond* (Cornell Univer-

sity, Ithaca, 1960).
[47] J. Junquera, M. Zimmer, P. Ordejón, and P. Ghosez, Phys. Rev. B **67**, 155327 (2003).
[48] K. Doll, Surf. Sci. **600**, L321 (2006).
[49] L. J. Vasek and J. M. Anderson, Proc. Phys. Soc. **73**, 733 (1959).
[50] J. H. Harding, Phys. Rev. B **32**, 6861 (1985).
[51] W. Humphrey, A. Dalke, and K. Schulten, J. Mol. Graphics **14**, 33 (1996).